

## Study of the Zirconium Isotopes with the $(p, t)$ Reaction\*

J. B. Ball and R. L. Auble

*Oak Ridge National Laboratory, Oak Ridge, Tennessee 37830*

and

P. G. Roos

*University of Maryland, College Park, Maryland 20742*

(Received 28 December 1970)

The  $(p, t)$  reaction has been studied on all stable isotopes of zirconium at a proton energy of 38 MeV. Triton spectra were analyzed with a magnetic spectrograph yielding over-all resolution on the order of 25 keV. Comparison of experimental angular distributions with two-nucleon transfer distorted-wave Born-approximation calculations is made to extract spin-parity assignments and transition enhancement factors for many of the observed levels. The observed  $L = 0$  transitions are discussed in terms of the shell model and the pairing-vibration model. The levels observed in  $^{88,89,90,92,94}\text{Zr}$  are compared with results of other experiments to derive a number of new level assignments. Measurements are also obtained of the one- and two-neutron binding energies from  $Q$  values deduced for the  $(p, t)$  and  $(p, d)$  ground-state transfer reactions.

### I. INTRODUCTION

In the past few years the importance of single-nucleon transfer reactions in determining the single-particle structure of nuclear levels has been demonstrated frequently. The transition strengths for these reactions are determined by the incoherent addition of the individual transition intensities from each shell-model orbital participating in the reaction. Thus, the single-nucleon transfer reactions yield important information on the magnitude of the single-particle components in the nuclear wave functions but are insensitive to the relative phases of the different components.

The transition strengths for two-nucleon transfer reactions, on the other hand, are determined by a coherent sum of the contributions from all possible pairs of particles. These strengths are thus quite sensitive to the phases of the various components of the wave functions but yield no direct information about individual magnitudes. Hence, results from such reactions can serve as an indication of the degree to which transitions to some states are enhanced over the strength expected from a single configuration, or in the case where model wave functions are available, can be used to examine the completeness and validity of the calculations.

This paper reports on a study of the zirconium nuclei with the two-neutron transfer  $(p, t)$  reaction. This reaction is particularly sensitive to the neutron structure of the nuclear wave functions but relatively insensitive to the proton structure. The stable zirconium isotopes span a region of 6 in neutron number beginning with the  $N = 50$  major

shell closure in  $^{90}\text{Zr}$ . Results from single-neutron transfer reaction studies indicate that beyond  $^{90}\text{Zr}$  the added neutrons occupy primarily the  $2d_{5/2}$  shell-model orbital.<sup>1</sup> The occupation of this orbital goes from effectively empty<sup>2</sup> for  $^{90}\text{Zr}$  to essentially full for  $^{96}\text{Zr}$ . The results from the present study are compared with the intensities expected from pure  $2d_{5/2}$  pair transfer as well as intensities predicted from shell-model calculations which provide a more complete description of the zirconium wave functions.

This work was partly motivated by the results of a study of the  $^{90}\text{Zr}(p, t)$  reaction reported previously.<sup>3</sup> In that reaction, the intensity of the  $L = 0$  transition leading to the ground state of  $^{88}\text{Zr}$  was found to be strongly enhanced, exhausting a major portion of the sum of the  $L = 0$  transfer strength expected for all the orbitals between  $N = 28$  and  $N = 50$ . The question then arises as to what happens to this strength as neutrons are added to the next major shell? If this same highly correlated state is observed as a "core" pickup from the heavier isotopes, it would possess the structure of a "pairing vibration."<sup>4-6</sup> The  $L = 0$  transition strengths observed in the present work thus have a direct bearing on the degree to which pairing vibrations are a fundamental collective mode of excitation for these nuclei.

Since only natural-parity states are allowed in the one-step  $(p, t)$  reaction process, each final level excited by pickup from an even target will have a unique  $L$  transfer. Assignment of  $L$ -transfer values then yields directly the spin-parity assignments for the observed final states. In the following sections comparisons will be made between

experimental angular distributions and distorted-wave calculations to provide such information.

## II. EXPERIMENTAL RESULTS

The reactions were studied at a proton energy of 38 MeV. The proton beam was obtained from the Oak Ridge isochronous cyclotron and the tritons were detected with nuclear emulsions in the broad-range magnetic-spectrograph facility.

The targets were rolled self-supported foils of isotopically enriched zirconium metal. The thickness and isotopic abundance of each target are given in Table I. The over-all experimental resolution observed was about 25 keV for the spectra from the even targets. The resolution for the  $^{91}\text{Zr}$  spectra, taken in a later run, was 15 keV.

In the previous study<sup>3</sup> of  $^{90}\text{Zr}(p, t)$  at an incident energy of 31 MeV, deuteron peaks from other zirconium isotopes present in the target were observed to overlap the triton spectra. Since this is the region we wish to examine for evidence of "core-pickup" states, the interference of strong deuteron groups from the heavier mass targets becomes a severe problem. The energy of 38 MeV for the present study was chosen to eliminate this problem by shifting the deuteron and triton groups away from each other in the spectrograph. It was also hoped that the higher reaction energy might favor higher angular momentum transfer. At 31 MeV, the highest-order transition observed was  $\Delta L = 5$  although transitions up to  $\Delta L = 8$  are expected in this region.

Examples of spectra obtained in the present study are shown in Fig. 1. The figure shows the energy spectrum observed, at a scattering angle of  $20^\circ$ , for each of the targets. The data are all plotted with a common abscissa which corresponds to the position of the particles along the spectrograph focal plane and hence to the triton momentum. The plot is almost equivalent to plotting each spectrum as a function of the reaction  $Q$ . With the data plotted as shown, peaks from isotopic target impurities occur at the same position in each spectrum. The presence of such impurities is

most apparent in the  $^{96}\text{Zr}(p, t)$  spectrum where the target contains significant amounts of the lighter isotopes.

Angular distributions for triton groups observed from  $(p, t)$  on the even zirconium isotopes are shown in Figs. 2–5. The curves shown in these figures are results of the calculations to be discussed in the following section.

Very careful attention was paid to accurate cross calibration of the target thickness so that meaningful comparisons of the yields from each isotope can be made. Exposures on a natural zirconium foil were made and the natural isotopic abundances used to relate the different isotopes to each other. The known abundances of other isotopes in the  $^{96}\text{Zr}$  target were used in the same manner. The high degree of consistency for the relative cross sections can be judged by examining the  $20^\circ$  points shown for each of the ground-state angular distributions in Figs. 2–5. From our analysis, the relative intensities for the different targets are estimated to be accurate to 2–3% while the absolute cross sections have an uncertainty of about 10%. The major sources of the estimated error in the absolute cross sections are the determination of the solid angle of the spectrograph and uncertainty in absolute charge collection.

Since we observe the  $(p, d)$  ground-state transitions in our triton spectra, it is possible to get a simultaneous measurement of reaction  $Q$  values for one- and two-neutron transfer. The measured  $Q$  values and the one- and two-neutron binding energies derived therefrom are listed in Table II. Also shown in the table are the corresponding values from the mass spectrometer measurements of Ries, Damerow, and Johnson,<sup>7</sup> from the 1964 Atomic Mass Table,<sup>8</sup> and from a preliminary version of the 1970 Atomic Mass Adjustment.<sup>9</sup>

The absolute calibration of our spectrograph system has an uncertainty of order 100 keV. The final adjustment of the values given in Table II was accomplished by requiring internal consistency of the overdetermined quantities. Specifically, the requirements were that the  $B(n)$  for  $^{90}\text{Zr}$  and  $^{91}\text{Zr}$  sum to the  $B(2n)$  for  $^{91}\text{Zr}$  and the  $B(n)$  for  $^{91}\text{Zr}$  and  $^{92}\text{Zr}$  sum to the  $B(2n)$  for  $^{92}\text{Zr}$ . These two conditions can be met to within about 5 keV. In the work of Ries, Damerow, and Johnson,<sup>7</sup> the values of  $B(n)$  for  $^{91}\text{Zr}$  and  $^{92}\text{Zr}$  and the  $B(2n)$  for  $^{92}\text{Zr}$  were also overdetermined. Their three well-established quantities are seen to be in excellent agreement with our values and lend support to our choice of over-all normalization. We estimate the uncertainty in our normalization at about twice the uncertainty in the relative energies, i.e., about  $\pm 10$  keV.

TABLE I. Nominal thicknesses and isotopic abundances of targets.

| Target           | Thickness<br>(mg/cm <sup>2</sup> ) | Composition<br>(at.%) |                  |                  |                  |                  |
|------------------|------------------------------------|-----------------------|------------------|------------------|------------------|------------------|
|                  |                                    | $^{90}\text{Zr}$      | $^{91}\text{Zr}$ | $^{92}\text{Zr}$ | $^{94}\text{Zr}$ | $^{96}\text{Zr}$ |
| $^{90}\text{Zr}$ | 0.29                               | 97.80                 | 0.95             | 0.65             | 0.49             | <0.1             |
| $^{91}\text{Zr}$ | 0.25                               | 4.95                  | 91.85            | 2.51             | 0.62             | 0.07             |
| $^{92}\text{Zr}$ | 0.28                               | 2.86                  | 1.29             | 94.57            | 1.15             | 0.14             |
| $^{94}\text{Zr}$ | 0.56                               | 1.67                  | 0.42             | 0.76             | 96.93            | 0.22             |
| $^{96}\text{Zr}$ | 0.46                               | 9.19                  | 2.02             | 27.20            | 4.22             | 57.36            |

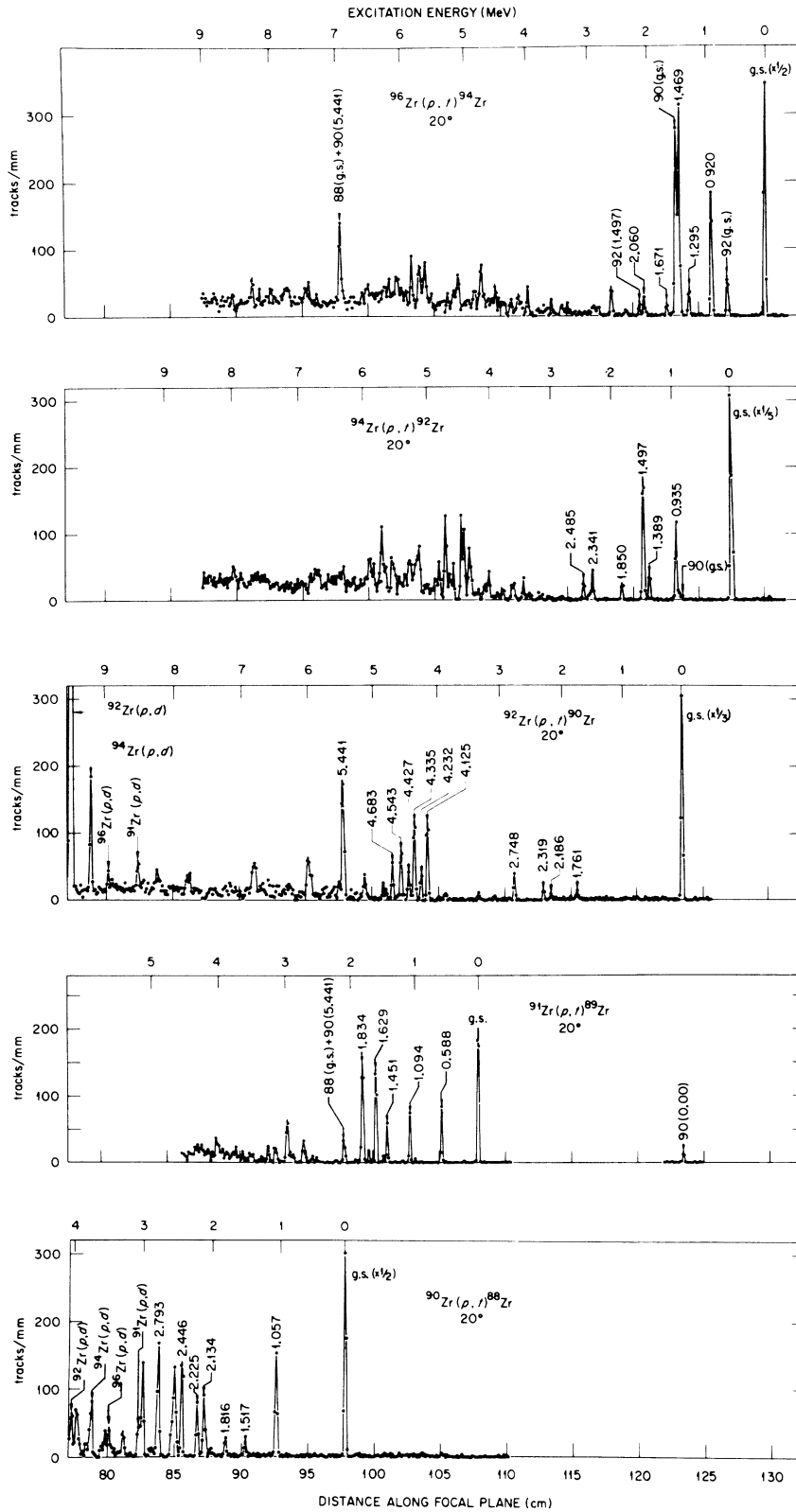


FIG. 1. Energy spectra of tritons observed at a scattering angle of  $20^\circ$  from the interaction of 38-MeV protons with all the stable zirconium isotopes.

The only appreciable discrepancy in the table seems to involve the  $B(n)$  for  $^{90}\text{Zr}$ . The present work indicates that the accepted value for this quantity is somewhat too large. This same error is also reflected in the disagreement for the value of  $B(2n)$  for  $^{91}\text{Zr}$ . Smaller disagreements are noted for the  $^{94}\text{Zr}$  and  $^{96}\text{Zr}$  values of  $B(n)$ . The good agreement for the values of  $B(2n)$  for these same nuclei suggests some adjustment of the  $^{93}\text{Zr}$  and  $^{95}\text{Zr}$  masses is needed.

### III. ANALYSIS

Calculations for the  $\text{Zr}(p, t)$  reactions were carried out in the distorted-wave Born approximation (DWBA) assuming a zero-range interaction between the proton and the center of mass of the two neutrons. The DWBA formalism for two-particle transfer reactions has been discussed in detail in the literature.<sup>10</sup> The calculations reported here were performed with the code JULIE.<sup>11</sup>

A general expression relating the experimental two-nucleon pickup cross section to the output of the JULIE program is

$$\sigma_J^{\text{exp}}(\theta) = \mathcal{G} \left\{ \frac{2\nu a^2(S)}{2S+1} \right\} C^2 D_0^2 \times \left| \sum_{j_1 j_2} B(j_1 j_2 J) \tilde{\beta}_{\text{JULIE}}(j_1 j_2 J, \theta) \right|^2, \quad (1)$$

where  $\tilde{\beta}(j_1 j_2 J, \theta)$  represents the complex transition amplitude calculated by the JULIE code for transfer of a pair of particles coupled to a resultant angular momentum  $J$ . The symbol  $B(j_1 j_2 J)$  is used for the nuclear two-particle spectroscopic amplitude in analogy to the same quantity defined by Yoshida.<sup>12</sup> It represents the probability that the initial and final wave functions differ only by a specific pair of particles, coupled to angular momentum  $J$ , multiplied by the total number of pairs of such particles available. For a single configuration in  $j$ - $j$  coupling,

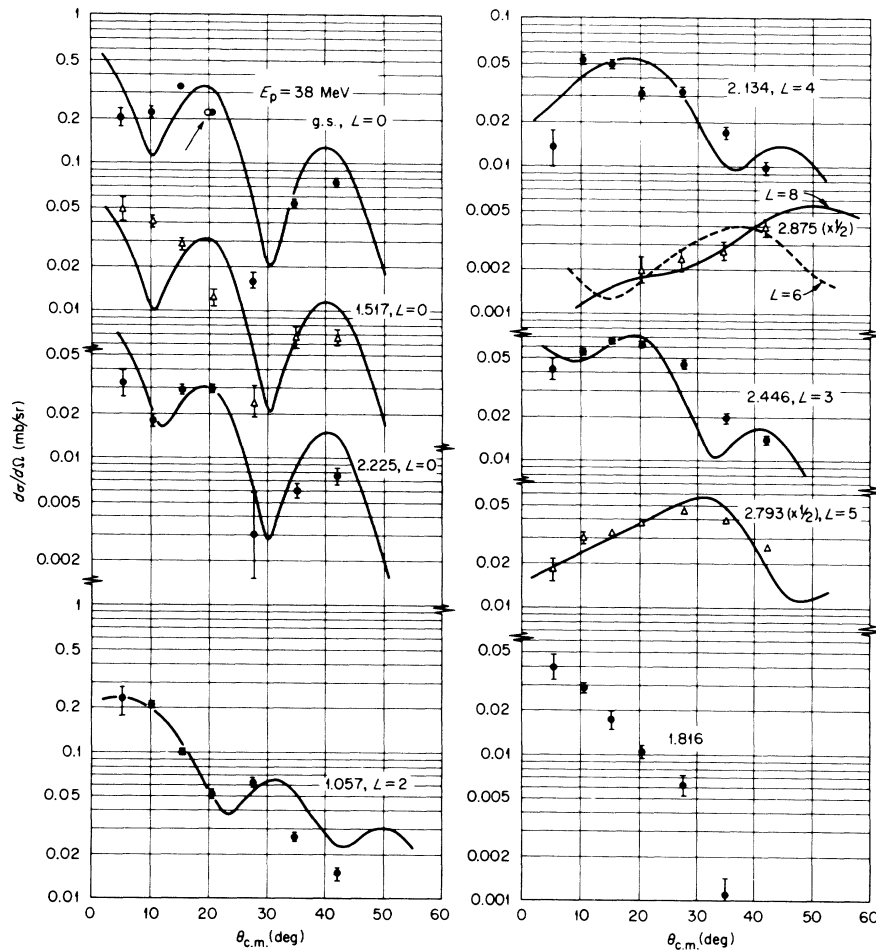


FIG. 2. Angular distributions for the triton groups observed in the  $^{90}\text{Zr}(p, t)^{88}\text{Zr}$  reaction. For the ground-state transition, the closed circles are data from the separated isotope target and the open circle at  $20^\circ$  (see arrow) is from the natural-target data. The curves are results of DWBA calculations for the indicated  $L$ -transfer values.

$$B(j^2, J) = \left( \frac{n(n-1)}{2} \right)^{1/2} [j^{n-2}(J, j^2(J) J_i) j^n J_i], \quad (2)$$

where the quantity in square brackets is the two-particle coefficient of fractional parentage.<sup>13</sup> The

usual method of running the JULIE program for multiconfiguration wave functions is to input the appropriate values of  $B(j_1 j_2 J)$ . The code performs the sum over  $j_1$  and  $j_2$  pairs and outputs the quantity that appears as the square of an absolute

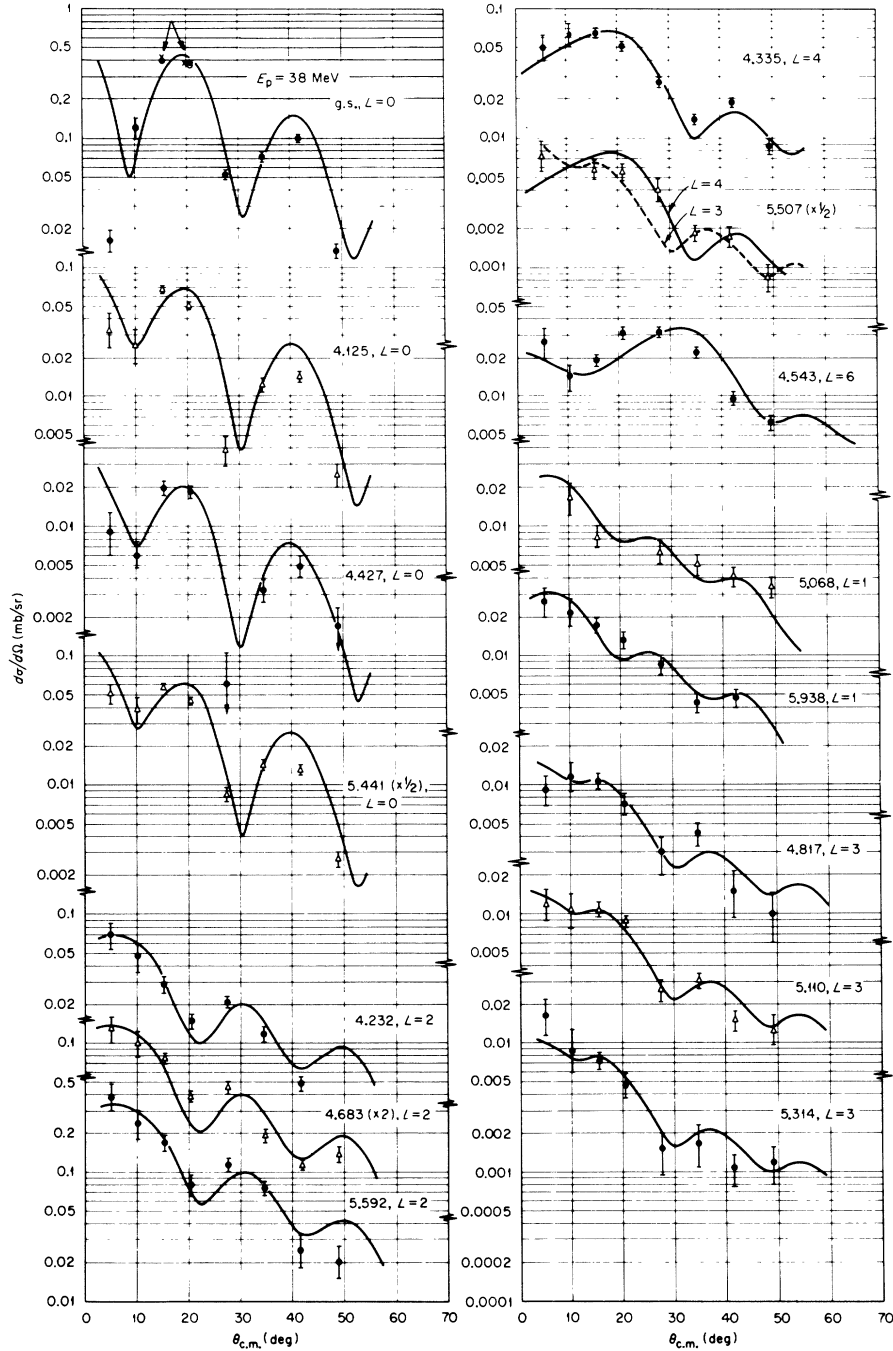


FIG. 3. Angular distributions for the triton groups observed in the  $^{92}\text{Zr}(p,t)^{90}\text{Zr}$  reaction. For the ground-state transition, the closed circles are data from the separated isotope target, the open circle (see arrow) is from the natural-target data, and the crosses (see arrow) are from the  $^{96}\text{Zr}$  target data. The curves are results of DWBA calculations for the indicated  $L$ -transfer values.

value in Eq. (1). Note that several quantities that appear externally in the equations of Refs. 10 and 12 are absorbed into the  $\tilde{\beta}(j_1 j_2 J)$  calculated by the JULIE code, the most obvious of these being the  $L$ - $S$  to  $j$ - $j$  recoupling coefficient.

The remaining quantities in Eq. (1) are external to the code and affect only the absolute normalization. The factor  $C^2$  is the square of the isospin coupling coefficient and  $D_0^2$  is the normalization factor which arises in making the zero-range approximation. For the JULIE program,  $D_0^2$  is in units of  $1.0028 \times 10^4 \text{ MeV}^2 \text{ F}^3$ . The factor  $\nu a^2(S)$  is equivalent to a spectroscopic factor for the light-particle system, with  $a^2(S)$  being the probability for finding two particles in a state with spin  $S$  and  $\nu$  the number of such pairs present in the light-particle system. For a  $(p, t)$  reaction it is assumed that the neutron pair in the triton can be treated as a pure  $S=0$  pair. Thus  $a^2(S)$  is unity for this light-particle system, and the quantity in brackets in Eq. (1) reduces to the factor of 2 for

the  $(p, t)$  reaction. This is the origin of the factor of 2 shown in the cross-section expression of Ref. 3.

Finally, we introduce a quantity  $\mathcal{E}$  which we call the "enhancement factor." This enhancement factor replaces the spectroscopic factor in the similar expression for single-nucleon transfer reactions and differs mainly in that it appears outside the sum over the participating shell-model orbitals. The enhancement factor will be used to compare experimental intensities with those calculated on the basis of specific assumptions about the nuclear wave functions involved. Disagreement between theory and experiment is indicated by deviations of the "enhancement factor" from unity.

The single-particle wave functions for the transferred neutrons were calculated in a Woods-Saxon well, by means of an oscillator wave-function expansion over the principle quantum number.<sup>14</sup> The use of 10 terms in the expansion was sufficient to insure accuracy in the calculations. The param-

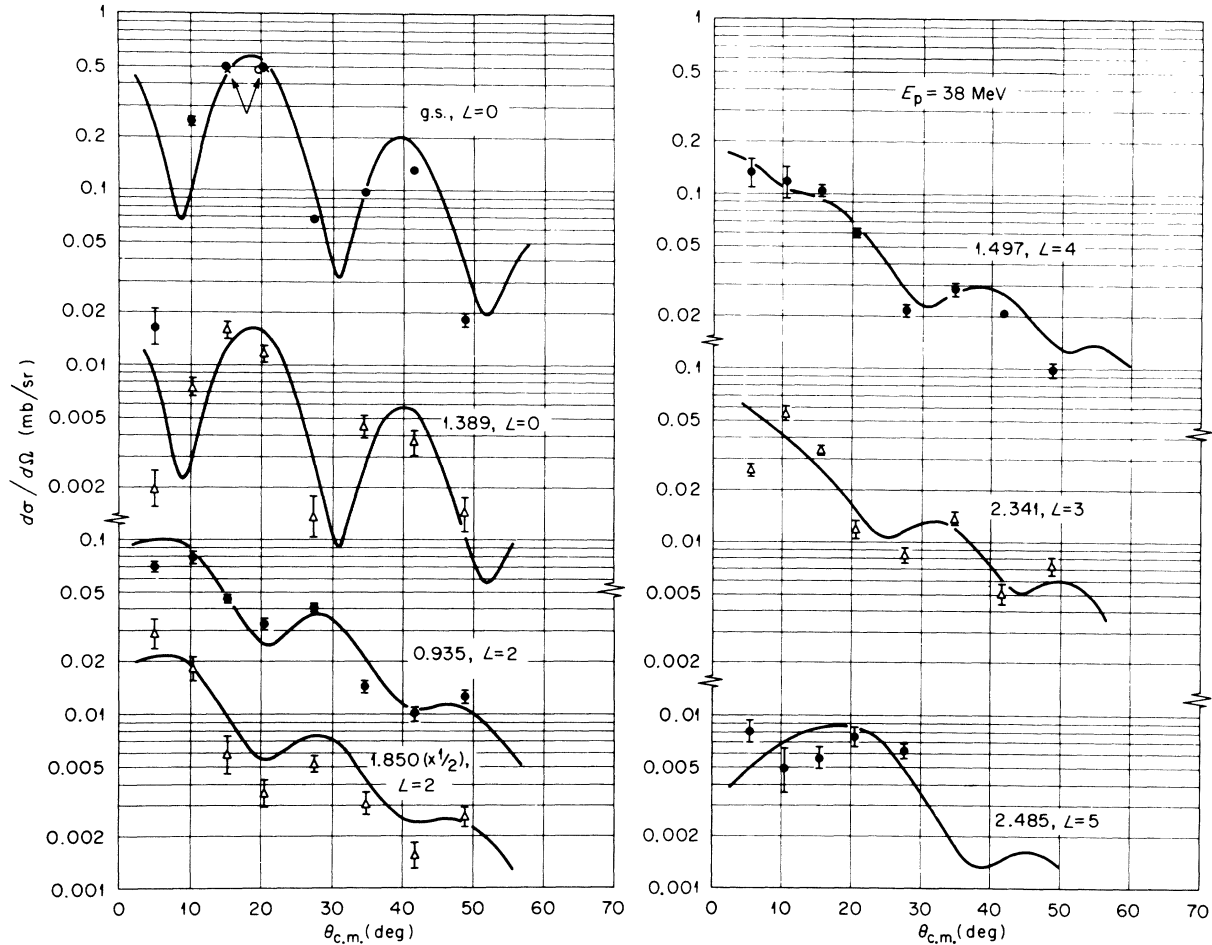


FIG. 4. Angular distributions for the triton groups observed in the  $^{94}\text{Zr}(p, t)^{92}\text{Zr}$  reaction. The same remarks apply as for Fig. 3.

ters for the Woods-Saxon well were a real well radius parameter of  $r_0 = 1.25$  and a diffusivity of  $a = 0.65$ . A Thomas-type spin-orbit term was used which had the same geometry and a strength of  $\lambda = 25$ . The binding energy for each neutron was taken to be one-half the two-neutron separation energy.

Previous analyses of two-nucleon transfer reactions<sup>3,15</sup> have shown the DWBA calculations to be sensitive to the choice of optical-model potentials. Therefore, a number of calculations were performed using different optical-model potentials which fit the available elastic scattering data.

The proton optical-model parameters were taken from the average sets of Blumberg *et al.*,<sup>16</sup> Fricke *et al.*,<sup>17</sup> and Becchetti and Greenlees (B-G).<sup>18</sup> The first two sets were obtained from an analysis of 40-MeV proton elastic scattering including polarization. The potentials of B-G were obtained from a global analysis of all available elastic scattering data for  $A > 40$  and  $E < 50$  MeV, including the data of Ref. 16. We tried two sets of potentials from the B-G analysis; one characterized by a real well radius of  $r_0 = 1.12$  and the other by  $r_0 = 1.17$ . The potentials from this analysis have the advantage that the energy dependence of

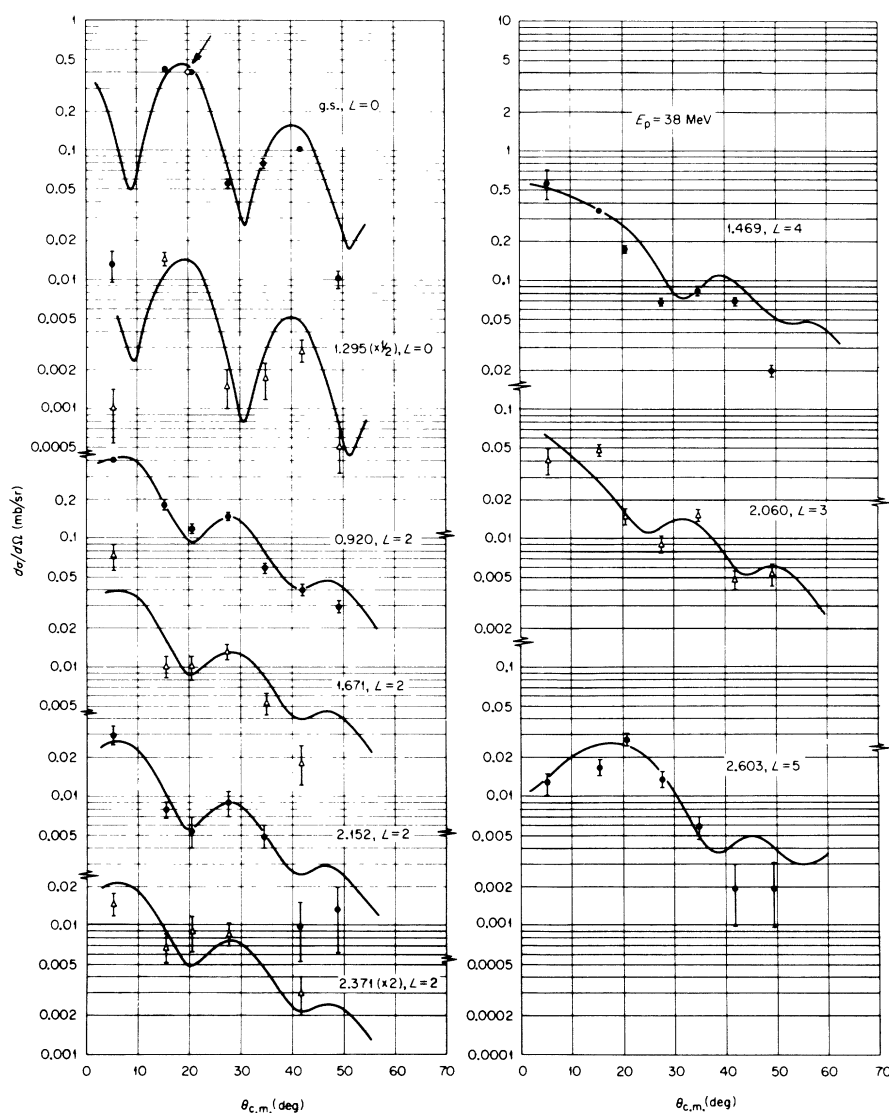


FIG. 5. Angular distributions for the triton groups observed in the  $^{96}\text{Zr}(p,t)^{94}\text{Zr}$  reaction. The same remarks apply as for Fig. 2.

the parameters is given, and can thus be used in the analysis of a wide range of reactions, leading to more consistent results.

The triton potentials were taken from an analysis by Drisko, Roos, and Bassel<sup>19</sup> of 20-MeV triton elastic scattering from  $^{90}\text{Zr}$ . Since the energy dependence of  $^3\text{He}$  optical potentials appears to be quite small,<sup>20</sup> these triton potentials should be suitable for our analysis. Three sets of triton parameters, which give equivalent fits to the elastic scattering, were chosen from those of the  $Vr$  continuous ambiguity. These were characterized by real well radii of  $r_0 = 1.08, 1.15,$  and  $1.24$ .

From calculations done for the  $0^+, 2^+,$  and  $4^+$  states using different optical-model potentials, we found relatively small changes in the shape of the angular distributions, leading to no strong preference for any particular potential. The different proton potentials did lead to some magnitude dependence in the cross sections (up to 25%), but the relative cross sections for  $0^+, 2^+,$  and  $4^+$  transitions changed by less than 10%. Since the energy dependence of the parameters is given by B-G, we calculated the  $^{90,92,94}\text{Zr}(t, p)$  reactions for their two sets of proton potentials and compared them to the 20-MeV data of Beery.<sup>21</sup> In this case there is some preference for the  $r_0 = 1.12$  parameters, which we then used in all subsequent calculations. These parameters are listed in Table III.

Somewhat surprisingly, calculations performed with different sets of triton parameters from the continuous ambiguity showed essentially no change

in the shape of the calculated angular distribution. This is in contrast to the 30-MeV  $^{90}\text{Zr}(p, t)^{88}\text{Zr}$  calculations which showed sensitivity in shape to the triton parameters.<sup>3</sup> Although no large shape change was observed for the different triton parameters, there is a rather large effect on the magnitudes of the calculated cross sections, including the relative magnitudes for different  $L$  transfers. Performing DWBA calculations for several parameter sets along the continuous ambiguity, we find that in going from the set with  $r_0 = 1.24$  to the set with  $r_0 = 1.08$  the calculated cross section for the  $0^+$  state increases by a factor of 2.4 while that for the  $4^+$  state increases by only a factor of 1.5. Thus, this effect can lead to rather large uncertainties in the relative spectroscopic factors. Because our previous results at 30 MeV showed a strong preference for the parameter set with  $r_0 = 1.15$ , and because single-particle transfer reactions also prefer a radius parameter of approximately this size, we have carried out all of our calculations with this set. The parameters for the triton potential are listed in Table III.

A comparison of the DWBA calculations to all of the experimental data is shown in Figs. 2–5. Overall, the fit to the data is rather good, giving one some confidence in the DWBA calculations. There are several discrepancies which are apparent in this comparison. First, the  $0^+$  calculated angular distribution is shifted about 2 to 3° from the experimental data. This is not a serious discrepancy, and is rather common in two-nucleon transfer analyses. We found that by artificially increasing the real well depth of the proton optical potential by about 4 MeV (~7%) we could shift the calculated angular distribution by the required amount. We have not done this in the calculations shown in the figures, since there is no justification for this pro-

TABLE II. Comparison of one- and two-neutron binding energies determined from the present study with previous mass studies. Energies are in MeV with errors in keV shown as superscripts. Errors for the present study are estimated not to exceed 10 keV.

| Nucleus          | This experiment |         | Previous determinations |                     |                     |
|------------------|-----------------|---------|-------------------------|---------------------|---------------------|
|                  | $Q(p, d)$       | $B(n)$  | $B(n)^a$                | $B(n)^b$            | $B(n)^c$            |
| $^{90}\text{Zr}$ | -9.728          | 11.953  | ...                     | 11.997 <sup>6</sup> | 11.983 <sup>4</sup> |
| $^{91}\text{Zr}$ | -4.977          | 7.202   | 7.210 <sup>7</sup>      | 7.194 <sup>5</sup>  | 7.203 <sup>3</sup>  |
| $^{92}\text{Zr}$ | -6.410          | 8.635   | 8.633 <sup>6</sup>      | 8.640 <sup>5</sup>  | 8.635 <sup>2</sup>  |
| $^{94}\text{Zr}$ | -6.000          | 8.225   | ...                     | 8.198 <sup>6</sup>  | 8.191 <sup>5</sup>  |
| $^{96}\text{Zr}$ | -5.630          | 7.855   | ...                     | 7.838 <sup>7</sup>  | 7.831 <sup>6</sup>  |
|                  | $Q(p, t)$       | $B(2n)$ | $B(2n)^a$               | $B(2n)^b$           | $B(2n)^c$           |
| $^{90}\text{Zr}$ | -12.805         | 21.287  | ...                     | ...                 | 21.29 <sup>20</sup> |
| $^{91}\text{Zr}$ | -10.677         | 19.159  | ...                     | 19.191 <sup>7</sup> | 19.185 <sup>5</sup> |
| $^{92}\text{Zr}$ | -7.350          | 15.832  | 15.834 <sup>7</sup>     | 15.834 <sup>3</sup> | 15.838 <sup>3</sup> |
| $^{94}\text{Zr}$ | -6.470          | 14.952  | 14.941 <sup>6</sup>     | 14.948 <sup>3</sup> | 14.949 <sup>3</sup> |
| $^{96}\text{Zr}$ | -5.825          | 14.307  | 14.326 <sup>8</sup>     | 14.306 <sup>4</sup> | 14.306 <sup>4</sup> |

<sup>a</sup>Mass-spectrometer measurements, Ref. 7.

<sup>b</sup>1964 Atomic Mass Tables, Ref. 8.

<sup>c</sup>1970 Atomic Mass Adjustment, preliminary version, Ref. 9.

TABLE III. Optical-model parameters used in the DWBA calculations. The notation for the parameters is the same as that of Satchler [see G. R. Satchler, Nucl. Phys. A92, 273 (1967)]. Multiple values are for  $^{90}\text{Zr}$ ,  $^{92}\text{Zr}$ ,  $^{94}\text{Zr}$ , and  $^{96}\text{Zr}$ , respectively.

|             | Proton                     |  |  |  | Triton |
|-------------|----------------------------|--|--|--|--------|
| $V$ (MeV)   | 53.9, 54.3, 54.7, 55.1     |  |  |  | 170.1  |
| $r_0$ (F)   | 1.12                       |  |  |  | 1.15   |
| $a$ (F)     | 0.78                       |  |  |  | 0.739  |
| $W$ (MeV)   | 5.66                       |  |  |  | 19.0   |
| $W_D$ (MeV) | 3.63, 3.86, 4.09, 4.30     |  |  |  | 0.0    |
| $r'_0$ (F)  | 1.32                       |  |  |  | 1.515  |
| $a'$ (F)    | 0.588, 0.601, 0.614, 0.627 |  |  |  | 0.758  |
| $V_s$ (MeV) | 6.2                        |  |  |  | 0.0    |
| $r_s$ (F)   | 0.98                       |  |  |  | 0.0    |
| $a_s$ (F)   | 0.75                       |  |  |  | 0.0    |
| $r_c$ (F)   | 1.2                        |  |  |  | 1.4    |



cedure. However, it is encouraging that this procedure of increasing the depth of the proton potential produces a negligible change in the DWBA cross section at the maximum near  $18^\circ$ , which is used in the normalization to the data. Increasing the proton well depth produces only small changes in the  $2^+$  and  $4^+$  calculations.

A second discrepancy observed in the comparison of experimental and theoretical angular distributions is that the calculated minimum at  $5^\circ$  is not deep enough. From Fig. 1 we can see that experimentally the depth of this minimum increases in going from  $^{90}\text{Zr}$  to  $^{96}\text{Zr}$ . In an investigation of this feature, as well as the angular shift, we performed DWBA calculations which included the effect of the nonlocality of the optical potentials in the local energy approximation.<sup>22</sup> These corrections have the effect of damping the form factor in the nuclear interior, the same effect expected if one includes finite-range effects. The results of these calculations for the  $0^+$  states are shown in Fig. 6. For  $^{90}\text{Zr}(p, t)$  the nonlocal corrections produce small changes in the angular distribution. For  $^{96}\text{Zr}(p, t)$  the minimum at  $5^\circ$  is more pronounced and in better agreement with the experimental data. Also there is a slight shift inward of

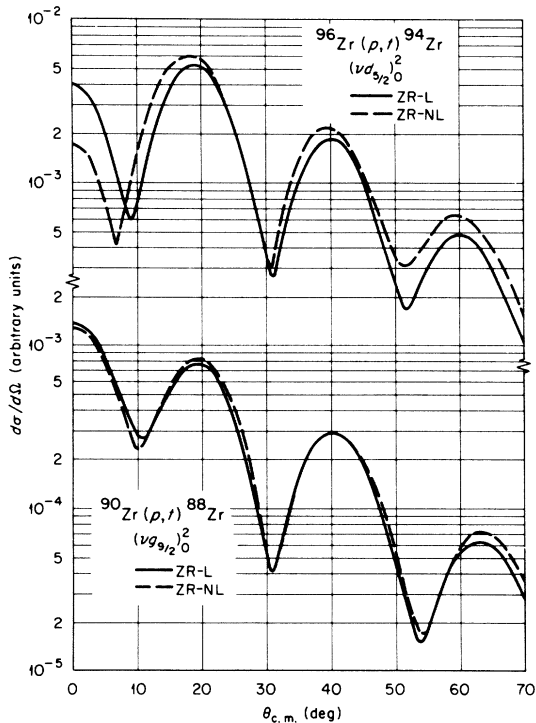


FIG. 6. Calculated angular distribution for two  $L=0$  transitions comparing results of the local zero-range calculations with the same calculations corrected for nonlocality effects.

the theoretical angular distribution. Thus, it appears that the discrepancies observed between theory and experiment for  $L=0$  transitions might be explained by nonlocal and finite-range effects. The nonlocal corrections were also tried for the  $2^+$  and  $4^+$  states and found to have negligible effects. Since the peak cross sections change only by small amounts in the calculations presented here, we feel that the extraction of spectroscopic information using zero-range, local calculations should be quite adequate.

The curves exhibited in Figs. 2–5 have been calculated for the single configuration expected to dominate the particular transition displayed. For example, the  $^{92,94,96}\text{Zr}(p, t)$  transitions to low-lying states have been calculated assuming the transfer of two  $2d_{5/2}$  neutrons. A nice feature of the calculations for this experiment is that the DWBA angular distributions for a particular  $J^\pi$  are essentially identical in shape for all configurations considered. This is presumably related to the strong absorption of the particles, particularly the triton, so that the DWBA calculation is only sensitive to the tail of the form factor. Thus, even the mixed configuration wave functions discussed in the next section produce the same shape for the theoretical angular distributions as those shown in the figures.

In Tables IV–VIII we present the ratio of the experimental to the theoretical cross sections assuming a single configuration for the nuclear wave functions. The assumed transition for each state is listed in the table. In order to make this comparison it was necessary to choose the normalizing constant  $D_0^2$ , which is introduced when one makes the zero-range approximation. This constant is essentially unknown. To assign this constant we have compared the magnitude of our experimental angular distributions to calculations done with wave functions from an extended shell-model calculation. The results of these calculations are presented in the next section. By requiring over-all consistency we arrived at a value of  $D_0^2 = 22$  which was then used to obtain the enhancement factors listed in the tables. This  $D_0^2$  is smaller than that reported in our previous paper<sup>3</sup> (37.5). This difference is accounted for by the fact that we used a larger bound-state radius ( $r_0 = 1.25$ ) in the present analysis than previously ( $r_0 = 1.20$ ). The larger bound-state radius produces approximately a factor of 2 increase in the DWBA cross section.

From Tables IV–VIII we can see that the  $0^+$  ground states are significantly enhanced over the simple  $(d_{5/2})^n$  description, whereas the  $2^+$  and particularly the  $4^+$  states are more reasonably predicted. It is obvious from this table that, even

TABLE IV. Levels in  $^{88}\text{Zr}$  observed with the  $^{90}\text{Zr}(p, t)$  reaction. The enhancements are extracted for a value of  $D_0^2=22$ . The listed spin-parity assignments are based on the present work and the previous data of Ref. 3.

| $E$ (MeV) | $J^\pi$                | $L$    | Assumed transition | $B^2(j_1 j_2 J)$ | $\mathcal{E}$ |
|-----------|------------------------|--------|--------------------|------------------|---------------|
| 0.000     | $0^+$                  | 0      | a                  | 1.0              | 10.0          |
| 1.057     | $2^+$                  | 2      | a                  | 5.0              | 3.4           |
| 1.517     | $0^+$                  | (0)    | a                  | 1.0              | 0.9           |
| 1.816     | ...                    | ...    | ...                | ...              | ...           |
| 2.134     | $4^+$                  | 4      | a                  | 9.0              | 1.2           |
| 2.225     | $0^+$                  | 0      | a                  | 1.0              | 1.1           |
| 2.446     | $3^-$                  | 3      | b                  | 7.0              |               |
| 2.6       | (Unresolved multiplet) |        |                    | ...              | ...           |
| 2.793     | $5^-$                  | 5      | b                  | 11.0             |               |
| 2.875     | $(8^+, 6^+)$           | (8, 6) | a                  | 17.0, 13.0       | 0.6, 0.35     |

$$^a (g_{9/2})_{0}^{10} \rightarrow (g_{9/2})_{J}^8.$$

$$^b [(p_{3/2})_{0}^4 (g_{9/2})_{0}^{10}]_0 - [(p_{3/2})_{3/2}^3 (g_{9/2})_{9/2}^9]_J.$$

considering  $D_0^2$  as a variable, consistency is lacking between the various states. Clearly more sophisticated nuclear wave functions are required.

#### IV. DISCUSSION

##### A. $L = 0$ Transitions

This class of reactions is particularly interesting since these transitions yield information on the nature of the pair correlations in nuclei and their effect on the nuclear wave functions. In terms of the pairing-vibration model, these zero-coupled pairs of particles represent the fundamental quanta of collective excitation for the system and our observed transitions thus provide a test of the predictions of this model.

TABLE V. Levels in  $^{89}\text{Zr}$  observed with the  $^{91}\text{Zr}(p, t)$  reaction. The enhancements are extracted for a value of  $D_0^2=22$ . The listed spin-parity assignments are based on the present work and the previous data summarized in Fig. 7.

| $E$ (MeV) | $J^\pi$                        | $L$ | Assumed transition | $B^2(j_1 j_2 J)$ | $\mathcal{E}$ |
|-----------|--------------------------------|-----|--------------------|------------------|---------------|
| 0.000     | $\frac{9}{2}^+$                | ... | ...                | ...              | ...           |
| 0.588     | $\frac{1}{2}^-$                | (3) | a                  | 1.17             | 0.9           |
| 1.094     | $\frac{3}{2}^-$                | ... | ...                | ...              | ...           |
| 1.451     | $\frac{5}{2}^-$                | ... | ...                | ...              | ...           |
| 1.512     | $\frac{7}{2}^+$                | ... | ...                | ...              | ...           |
| 1.629     | $\frac{5}{2}^+$                | (0) | b                  | 1.0              | 2.5           |
| 1.742     | $(\frac{3}{2}, \frac{1}{2})^-$ | ... | ...                | ...              | ...           |
| 1.834     | $(\frac{5}{2}^+)$              | (0) | b                  | 1.0              | 3.0           |
| 1.867     | $(\frac{3}{2}, \frac{1}{2})^-$ | ... | ...                | ...              | ...           |

$$^a [(p_{1/2})_{0}^2 (d_{5/2})_{5/2}]_{5/2} \rightarrow (p_{1/2}).$$

<sup>b</sup>See Table IV.

In a preliminary report of this work we presented a comparison of the observed  $L = 0$  transfer intensities.<sup>23</sup> The enhancement factors extracted from our DWBA analysis shown in Tables IV–VIII do not substantially affect our previous conclusions.

It has been shown previously that the  $N = 50$  shell closure at  $^{90}\text{Zr}$  is quite good and that a neutron pair is found to occupy orbitals in the next major shell with a probability of only about 3%.<sup>2</sup> Thus the enhancement factor of 10 observed for the  $(p, t)$  transition to the  $^{88}\text{Zr}$  ground state cannot be ascribed to two-particle-two-hole impurity components of the  $^{90}\text{Zr}$  ground state but instead implies a very coherent structure for the  $^{88}\text{Zr}$  ground state with significant two-hole components from the  $2p_{1/2}$  and  $2p_{3/2}$  orbitals. In fact this enhancement factor exhausts a major portion of the  $L = 0$  transition strength expected from all the orbitals comprising this major neutron shell. The fact that no strongly populated excited  $0^+$  states are observed supports this conclusion.

For the heavier zirconium isotopes, the simplest shell-model picture is to assume that the additional neutrons fill the  $2d_{5/2}$  orbital. The ground-state-to-ground-state reaction from the even targets is treated in Tables VI–VIII on the basis of pickup of a  $d_{5/2}$  neutron pair. It is interesting that the square of the nuclear spectroscopic amplitude,  $B^2(j_1 j_2 J)$ , introduces a ratio of 1.0 : 1.33 : 1.0 for the  $^{92}, ^{94}, ^{96}\text{Zr}$  reactions, respectively. This is almost exactly the observed experimental ratio of these ground-state cross sections. An examination of the extracted enhancements, however, shows that the  $Q$ -value dependence of the DWBA calculations results in deviations of the ground-state enhancements of about 10% from the average value. More importantly, the extracted enhancements are significantly larger than unity indicating that the simple  $d_{5/2}$  model cannot ac-

TABLE VI. Levels in  $^{90}\text{Zr}$  observed with the  $^{92}\text{Zr}(p, t)$  reaction. The enhancements are extracted for a value of  $D_0^2=22$ . The listed spin-parity assignments are based on the present work and the previous data summarized in Fig. 8.

| $E(\text{MeV})$ | $J^\pi$      | $L$    | Assumed transition | $B^2(j_1 j_2 J)$ | $\mathcal{E}$ |
|-----------------|--------------|--------|--------------------|------------------|---------------|
| 0.000           | $0^+$        | 0      | a                  | 1.0              | 1.6           |
| 1.761           | $0^+$        | 0      | a                  | 1.0              | 0.02          |
| 2.186           | $2^+$        | 2      | a                  | 1.0              | 0.13          |
| 2.319           | $5^-$        |        |                    |                  |               |
| 2.748           | $3^-$        |        |                    |                  |               |
| 4.125           | $0^+$        | 0      | b                  | 1.0              | 2.2           |
| 4.232           | $2^+$        | 2      | c                  | 1.67             | 0.3           |
| 4.335           | $4^+$        | 4      | c, b               | 3.0, 9.0         | 0.5, 1.4      |
| 4.427           | $0^+$        | 0      | b                  | 1.0              | 0.6           |
| 4.543           | $6^+$        | 6      | c                  | 4.33             | 0.45          |
| 4.683           | $2^+$        | 2      | c, b               | 1.67, 5.0        | 0.3, 1.0      |
| 4.817           | $3^-$        | 3      | d                  | 2.33             | 0.05          |
| 5.068           | $(1^-)$      | (1)    | e                  | 1.0              | 0.07          |
| 5.110           | $3^-$        | 3      | d, e               | 2.33, 2.33       | 0.09, 0.10    |
| 5.314           | $3^-$        | 3      | e                  | 2.33             | 0.03          |
| 5.441           | $0^+$        | 0      | b                  | 1.0              | 4.3           |
| 5.507           | $(3^-, 4^+)$ | (3, 4) | e, c               | 2.33, 3.0        | 0.06, 0.12    |
| 5.592           | $2^+$        | 2      | c                  | 1.67             | 0.16          |
| 5.938           | $(1^-)$      | (1)    | e                  | 1.0              | 0.09          |

<sup>a</sup>  $[(^{90}\text{Zr})_J(d_{5/2})^2_J]_0 \rightarrow (^{90}\text{Zr})_J$ .

<sup>b</sup> See Table IV.

<sup>c</sup>  $[(g_{9/2})^{10}_0(d_{5/2})^2_0]_0 \rightarrow [(g_{9/2})^9_{9/2}(d_{5/2})]_J$ .

<sup>d</sup>  $[(p_{1/2})^2_0(d_{5/2})^2_0]_0 \rightarrow [(p_{1/2})(d_{5/2})]_J$ .

<sup>e</sup>  $[(p_{3/2})^4_0(d_{5/2})^2_0]_0 \rightarrow [(p_{3/2})^3_{3/2}(d_{5/2})]_J$ .

count completely for the observed transition strengths. It is interesting to note that the extracted enhancements increase with target mass indicating the increased participation of other orbitals as neutrons are added.

In terms of the pairing-vibration model, these even zirconium ground states can be represented as one, two, and three particle pairs coupled to the  $^{90}\text{Zr}$  ground state. The ground-state transi-

TABLE VII. Levels in  $^{92}\text{Zr}$  observed with the  $^{94}\text{Zr}(p, t)$  reaction. The enhancements are extracted for a value of  $D_0^2=22$ . The listed spin-parity assignments are based on the present work and the previous data summarized in Fig. 9.

| $E(\text{MeV})$ | $J^\pi$ | $L$ | Assumed transition | $B^2(j_1 j_2 J)$ | $\mathcal{E}$ |
|-----------------|---------|-----|--------------------|------------------|---------------|
| 0.000           | $0^+$   | 0   | a                  | 1.33             | 1.7           |
| 0.935           | $2^+$   | 2   | a                  | 1.67             | 0.7           |
| 1.389           | $0^+$   | 0   | a                  | 1.33             | 0.05          |
| 1.497           | $4^+$   | 4   | a                  | 3.0              | 0.7           |
| 1.850           | $2^+$   | 2   | a                  | 1.67             | 0.3           |
| 2.341           | $3^-$   | (3) | b, c               | 4.67, 0.39       | 0.07, 1.3     |
| 2.386           | ...     | ... | ...                | ...              | ...           |
| 2.485           | $(5^-)$ | (5) | c                  | 0.61             | 0.3           |

<sup>a</sup>  $(d_{5/2})^4_0 \rightarrow (d_{5/2})^2_J$ .

<sup>b</sup>  $[(p_{3/2})^4_0(d_{5/2})^4_0]_0 \rightarrow [(p_{3/2})^3_{3/2}(d_{5/2})^3_{5/2}]_J$ .

<sup>c</sup>  $[(d_{5/2})^2_0(h_{11/2})^2_0]_0 \rightarrow [(d_{5/2})(h_{11/2})]_J$ .

tions thus represent the simplest vibrational transition of the system – the annihilation of one vibrational quanta. The very simple harmonic form of the model would predict transition intensity ratios proportional to the number of quanta in the initial state, i.e., a ratio of 1:2:3 for the  $^{92,94,96}\text{Zr}$  ground-state reactions. Values for the experimentally free of configuration assumptions but corrected for  $Q$ -value effects, can be obtained from the product  $\mathcal{E}B^2(j_1 j_2 J)$ . Appropriate renormalization yields a ratio of 1.0:1.4:1.2 for the experimental  $^{92,94,96}\text{Zr}$  ground-state transition intensities. It is obvious that the simple form of the model does not reproduce the observed ratio.

A more complete treatment of the pairing-vibration model for these nuclei, including effects of certain anharmonic correlations, has been given by Sørensen.<sup>24</sup> The ratio reported for the calculated ground-state transitions is 1.0:1.42:1.54. Thus the change from  $^{92}\text{Zr}$  to  $^{94}\text{Zr}$  is reproduced almost exactly but the trend from  $^{94}\text{Zr}$  to  $^{96}\text{Zr}$  is in the wrong direction. The experimental transition intensities seem to be intermediate between the predictions of the pure  $(d_{5/2})^n$  picture and the results of Sørensen. This would seem to suggest that while the  $(d_{5/2})^n$  model is not adequate for a complete description of the ground-state transitions, this orbital retains a dominant effect on the neutron portion of these ground-state wave

functions. It appears that the neutrons are not sufficiently spread over the orbitals of the valence shell to allow a good description of these transitions in terms of the pairing-vibration model.

*Note in proof:* In quoting the cross-section ratios predicted by the pairing-vibration model calculations of Sørensen, we have used his approximate values obtained by summing the squared  $G$  factors (in the notation of Ref. 10). Sørensen discusses the possible failings of such an approximation and performs DWBA calculations for our zirconium data. His results show the same general trend as our experimental ratios. In contrast, in our calculations for these zirconium data, we have found the summed and squared  $G$  factors to be a good estimate of relative cross sections. We have chosen to quote these since we feel they are related more closely to the model calculations.

One of the motivations for the present study was to examine the effect of valence neutrons on the strongly enhanced pickup observed from the  $N = 50$  closed shell. If this interaction is very small we might expect to observe such a core-pickup state in all the heavier isotopes at about the same position as the ground-state transition for the  $^{90}\text{Zr}(p, t)$  reaction. This resulting state, which is produced by creating a highly correlated hole pair in the neutron core while leaving the correlated particle pairs in the valence shell undisturbed, has the configuration which is usually referred to as "the pairing vibration" for the nucleus in question. In terms of the pairing-vibration model this state is described as particle-pair, hole-pair (i.e., one quantum of each type) excitation of the ground state.

TABLE VIII. Levels in  $^{94}\text{Zr}$  observed with the  $^{96}\text{Zr}(p, t)$  reaction. The enhancements are extracted for a value of  $D_0^2 = 22$ . The listed spin-parity assignments are based on the present work and the previous data summarized in Fig. 10.

| $E(\text{MeV})$ | $J^\pi$ | $L$ | Assumed transition | $B^2(j_1 j_2 J)$ | $\mathcal{E}$ |
|-----------------|---------|-----|--------------------|------------------|---------------|
| 0.000           | $0^+$   | 0   | a                  | 1.0              | 2.0           |
| 0.920           | $2^+$   | 2   | a                  | 5.0              | 0.9           |
| 1.295           | $0^+$   | 0   | a                  | 1.0              | 0.1           |
| 1.469           | $4^+$   | 4   | a                  | 9.0              | 0.8           |
| 1.671           | $2^+$   | 2   | a                  | 5.0              | 0.08          |
| 2.060           | $3^-$   | 3   | b, c               | 7.0, 0.78        | 0.05, 0.8     |
| 2.152           | $2^+$   | 2   | a                  | 5.0              | 0.05          |
| 2.371           | $2^+$   | 2   | a                  | 5.0              | 0.02          |
| 2.603           | $5^-$   | 5   | c                  | 1.22             | 0.5           |

$$^a (d_{5/2})_0^6 \rightarrow (d_{5/2})_J^4.$$

$$^b [(p_{3/2})_0^4 (d_{5/2})_0^6]_0 \rightarrow [(p_{3/2})_{3/2}^3 (d_{5/2})_{5/2}^5]_J.$$

$$^c [(d_{5/2})_0^4 (h_{11/2})_0^2]_0 \rightarrow [(d_{5/2})_{5/2}^3 (h_{11/2})_J].$$

Examination of the even target spectra in Fig. 1 reveals an excited state in the  $^{92}\text{Zr}(p, t)$  reaction that occurs at the expected energy for the "core-pickup" state (5.44 MeV) and, from Table VI, exhibits  $L = 0$  character. Although this peak dominates the spectrum in this region, it has less than half the strength of the  $^{90}\text{Zr}(p, t)^{88}\text{Zr}$  (g.s.) transition. No such single state is apparent in spectra from the  $^{94}\text{Zr}$  and  $^{96}\text{Zr}$  targets. The peak at the appropriate position in the  $^{96}\text{Zr}$  spectrum is due to the presence of  $^{90}\text{Zr}$  and  $^{92}\text{Zr}$  in the  $^{96}\text{Zr}$  target.

The calculations of Sørensen predict the pairing vibration in  $^{90}\text{Zr}$  should be populated with 70% of the intensity observed for the  $^{90}\text{Zr}(p, t)^{88}\text{Zr}$  ground-state transition. The reduction to 70% comes from inclusion of anharmonic effects. While we observe experimentally only 43% of the strength to the 5.44-MeV level, two other  $L = 0$  transitions are observed in this same region of excitation. The total transition strength to all three levels is 71% in excellent agreement with the model predictions. The discrepancy remains, however, that the strength is spread over at least three levels.

We are unable to ascertain if further fragmentation occurs for the  $^{94}\text{Zr}$  and  $^{96}\text{Zr}$  reactions in analogy with a similar study of the Nd isotopes.<sup>25</sup> The combination of high level density and lack of an easily identifiable feature for the  $L = 0$  transitions at this energy make it impossible to extract reliable information from these spectra.

Although spectra at only two angles were obtained from the  $^{91}\text{Zr}$  target, transitions dominated by  $L = 0$  transfer will show a sharp rise from 10 to 20° while other  $L$  transfers will not. The only two levels observed to have this character are shown in Table V to be separated by only 200 keV and to be populated with almost equal intensity.

We thus conclude that while we do observe pickup strength attributable to removal of neutron pairs from the  $N = 50$  core, the transfer strength to the strongly correlated state observed in the  $^{90}\text{Zr}(p, t)$  reaction, is rapidly fractionated as neutrons are added to the next major shell. It would appear that the presence of these "valence" neutrons causes significant changes in the correlations between the "core" neutrons.

#### B. Levels in $^{88}\text{Zr}$

The properties of the  $^{88}\text{Zr}$  levels listed in Table IV are in good agreement with those reported previously<sup>3</sup> from a study of the same reaction at a proton energy of 31 MeV. In particular, the good agreement between the enhancements extracted at the two energies gives some indication that the DWBA calculations are done in a consistent

manner.

In the 31-MeV data, a group of levels near 2.6 MeV of excitation was not cleanly resolved. Part of the difficulty appeared to be due to the presence of one or more weak deuteron groups in the same region of the spectrograph focal plane. In the present work, this region of the triton spectra is still very complex even though raising the energy to 38 MeV has completely eliminated the presence of any deuteron groups. It appears that there are at least four levels in this multiplet within an energy span of about 70 keV.

Although the increase in reaction energy has removed the deuteron contamination from the triton spectra, the effect on the angular structure for the various  $L$ -transfer values is detrimental. The  $L=0$  transitions no longer rise sharply at forward angles to provide a convenient signature for identifying this particularly interesting class of two-neutron transfers and the differences between the different higher  $L$  transfers are much less distinct than at 31 MeV. Some of the observed angular distributions, shown in Fig. 2 do not give the unambiguous choice for  $L$  transfer that was

found at the lower energy.

The 1.517-MeV level has the minimum at about  $30^\circ$  which is characteristic of all the  $L=0$  transitions that we observe, but has a significantly different slope at forward angles. This transition was very clearly  $L=0$  in the 31-MeV data. There is no evidence in the peak shape, at either energy, for a close-lying doublet at this position and no combination of the other  $L$  transfers observed gives a better fit than the pure  $L=0$  shape. Attempts to reproduce the observed shape by mixed-configuration calculations having large destructive interference were unsuccessful and only produced calculated angular distributions almost identical to the single-configuration  $L=0$  calculations.

The 1.816-MeV level is not fit well by any of the calculated  $L$ -transfer shapes. This level also had an anomalous angular distribution at 31 MeV that was approximated by assuming an unresolved  $2^+$ ,  $4^+$  doublet. Such an explanation does not seem to be supported by the present data. This level and the nearby 1.517-MeV anomalous  $L=0$  level are fairly weakly excited and it may be that the same mechanism is responsible for both these unusual

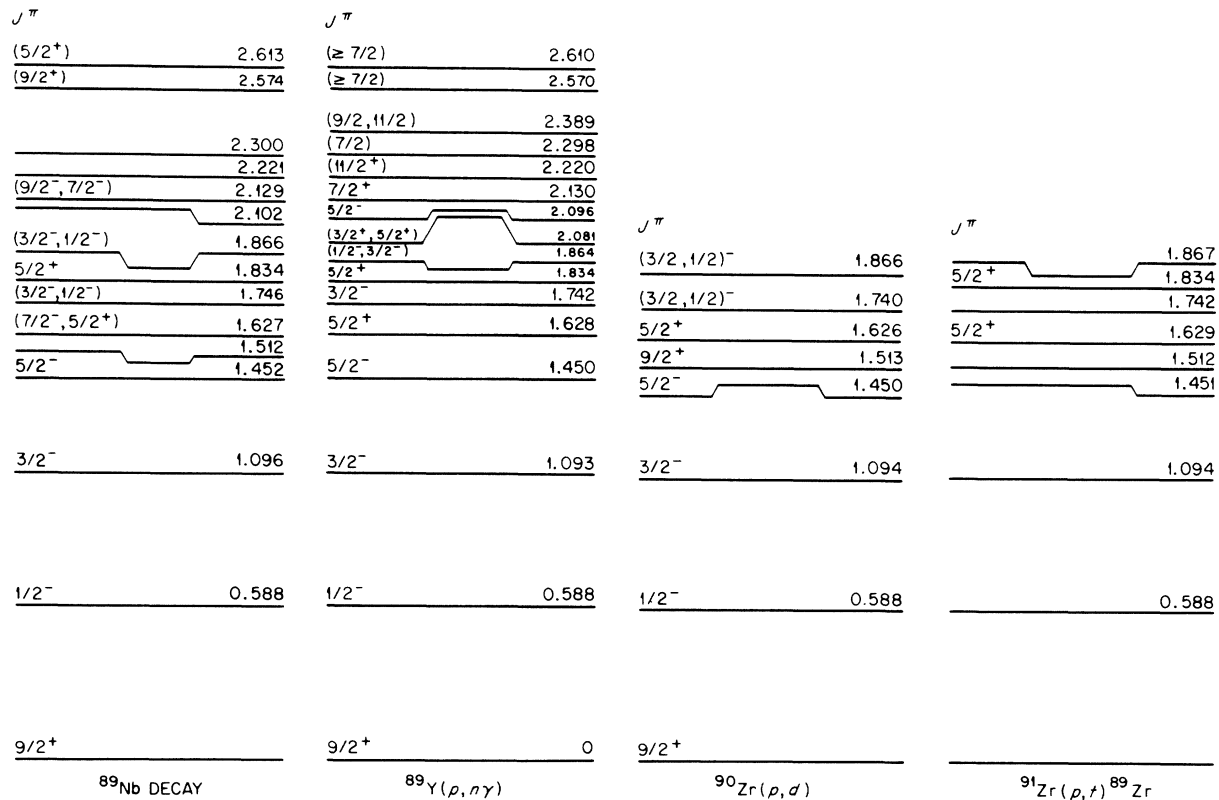


FIG. 7. Low-lying energy levels in  $^{89}\text{Zr}$ . The results of the present study are at the far right. The decay data are taken from Ref. 28, the  $(p, n\gamma)$  data from Ref. 29, and the  $(p, d)$  data from Ref. 2. In this figure, and those to follow, the spectra chosen for comparison are selected as representative of the data available and do not presume to be comprehensive.

angular distributions.

A level at 2.875 is seen clearly in the present study to have  $\Delta L \geq 6$ . Evidence for this level has also been reported in the study of  $^{88}\text{Nb}$  decay<sup>26</sup> and the study of the  $^{86}\text{Sr}(\alpha, 2n\gamma)$  reaction.<sup>27</sup> Those data favor an  $8^+$  assignment for this level.

#### C. Levels in $^{89}\text{Zr}$

Because we were interested primarily in studying the two-nucleon transitions between the even zirconium isotopes, spectra from the  $^{91}\text{Zr}$  target were obtained only at two angles (10 and 20°). Although the purpose of the spectra was to isolate any impurity peaks in the other spectra due to this reaction, there are a few interesting features observed.

The levels in  $^{89}\text{Zr}$ , listed in Table V are compared in Fig. 7 with levels observed in the decay<sup>28</sup> of  $^{89}\text{Nb}$ , in the  $^{89}\text{Y}(p, n\gamma)$  reaction,<sup>29</sup> and in the  $^{90}\text{Zr}(p, d)$  reaction.<sup>2</sup> As discussed in Sec. A, the transitions to levels at 1.629 and 1.834 MeV are tentatively assigned  $L=0$  character. Since the  $^{91}\text{Zr}$  ground state is  $\frac{5}{2}^+$ , an  $L=0$  transition implies  $\frac{5}{2}^+$  for these two states in  $^{89}\text{Zr}$ . The 1.629-MeV level has been assigned previously as  $\frac{5}{2}^+$  from results of the  $^{90}\text{Zr}(p, d)$  reaction.<sup>2</sup> This assignment is also consistent with the decay scheme and  $(p, n\gamma)$  results. The 1.834-MeV level was not seen in the  $(p, d)$  study but was observed in the other two studies and assigned as  $\frac{5}{2}^+$ . Our result confirms both of these levels as  $\frac{5}{2}^+$ .

The next higher excited state reported in the  $^{89}\text{Nb}$  decay study with possible  $\frac{5}{2}^+$  spin-parity is at 2.613 MeV of excitation. We see an excited state that probably corresponds to this level but its intensity is more than an order of magnitude weaker than the two lower  $\frac{5}{2}^+$  levels. Thus, very little of the  $L=0$  transition strength goes to this state if it is  $\frac{5}{2}^+$ . We see no evidence for the 2.081-MeV level reported as a possible  $\frac{5}{2}^+$  level in the  $(p, n\gamma)$  results nor was such a state reported in the  $^{89}\text{Nb}$  decay.

The transition to the 0.588-MeV level must be  $L=3$  since the state is well established as  $\frac{1}{2}^-$  and only an  $L=3$  transition is allowed.

#### D. Levels in $^{90}\text{Zr}$

Energy levels in  $^{90}\text{Zr}$  up to about 6 MeV of excitation have been analyzed in the present study and are compared in Fig. 8 with results of other experiments.<sup>30-32</sup>

From Fig. 1 it can be seen that the  $L=0$  ground-state transition dominates the lower-excitation portion of the spectrum. Up to about 4 MeV of excitation, only weak population of the excited states is observed. This feature of the  $(p, t)$  results

supports the assumed closed-neutron-shell nature of  $^{90}\text{Zr}$  and previous studies which have attributed the low-lying states to excitations of the proton structure. The strongest of the low-lying states is the 2.748-MeV level. This state is the well known  $3^-$  octupole vibration in this nucleus.<sup>33</sup> These results indicate some neutron-structure contribution to this collective state.

At about 4 MeV of excitation we begin to see levels populated with more intensity. It seems reasonable to assume that these states arise either from pickup of a pair of neutrons from the closed-shell orbitals or a pair made up from one of the core neutrons coupled to a valence neutron. This latter type of pickup would then leave the residual nucleus in a configuration described as a particle-hole excitation. If the valence pair of neutrons in the  $^{92}\text{Zr}$  target occupies the most energetically favored orbital, the  $2d_{5/2}$ , then the pickup of one of these neutrons and one of the  $g_{9/2}$  least-bound neutrons from the closed shell will result in a final state of the form  $(\nu g_{9/2})^{-1}(\nu d_{5/2})$ . This particle-hole coupling will produce a sextuplet of states ranging from  $2^+$  to  $7^+$ . Evidence for the existence of this multiplet in this region of excitation energy has been reported previously from a study of the  $^{91}\text{Zr}(p, d)$  reaction.<sup>2</sup> In that work, assignment of spin values to the observed sextuplet was made on the basis of transition intensities observed for the  $l=4$  single neutron transfer. These results are included in Fig. 8. Only the three normal-parity members of the sextuplet are allowed for the direct  $(p, t)$  reaction. The results of the present work confirm the  $2^+$  and  $4^+$  assignment for the levels at 4.232 and 4.335 MeV, respectively. The  $(p, d)$  work tentatively assigned a level at 4.53 MeV as  $7^+$  and a level at 5.05 MeV as  $6^+$ . These two levels were the most strongly populated and had nearly the same intensities. The present results indicate that this tentative assignment is incorrect and should be reversed. This reversal of  $6^+$ ,  $7^+$  assignment gives much better agreement with the theoretical calculations by Freed and Rhodes of the ordering of this particle-hole multiplet.<sup>34</sup> We place the  $6^+$  level at 4.543 MeV and, since we do not observe the higher level, it is most likely of non-normal parity and a  $7^+$  assignment is within the experimental uncertainties in the  $(p, d)$  work. These same two levels are also apparently observed in the decay of  $^{90}\text{Nb}$  and the choice of spin-parity assignments taken from the present study fall within the limits established from the decay scheme systematics.<sup>31, 32</sup> The results of the present work, when combined with results of other investigations of  $^{90}\text{Zr}$ , provide sufficient information to allow unique spin-parity assignments for almost all levels up to 5 MeV of ex-

citation. A summary of this information has been presented elsewhere.<sup>33</sup>

All three of the observed levels attributed to the particle-hole multiplet have, at most, half of the strength expected from the simple description of these levels. It would thus appear that other configurations are contributing destructively to these transfers. Although only six  $l=4$  transitions were observed in the  $(p, d)$  work, deviations from the  $2J+1$  intensity ratios, predicted by the simple particle-hole description, indicated the presence of some configuration mixing.

It is particularly interesting to note that we do not observe any indication of populating the non-

normal-parity members of the sextuplet. This is the only case in the present study where we have unambiguous assignment of non-normal-parity states to test this point. (The known  $4^-$  level<sup>33</sup> at 2.739 MeV would not be resolved from the 2.748-MeV collective  $3^-$  level.) As a specific example, at a scattering angle of  $27^\circ$  the  $2^+$ ,  $4^+$ , and  $6^+$  members of the particle-hole multiplet have nearly equal intensities. We observe 100, 124, and 145 counts, respectively, in the three peaks. At the position of the  $3^+$  and  $5^+$  levels determined from the  $(p, d)$  results we see no indication of peaks in the  $(p, t)$  spectrum. At these positions there are a maximum of 3 and 4 counts, respectively.

| $J^\pi$                                     | $\Delta L$                         | $J^\pi$                           | $J^\pi$   |
|---|------------------------------------|-----------------------------------|---|
| ----- 5.432                                 |                                    | <u>(1,2,3,4)<sup>-</sup> 5.42</u> | <u>0<sup>+</sup> 5.441</u>                      |
|   |                                    |                                   | <u>3<sup>-</sup> 5.314</u>                      |
| <u>(8<sup>+</sup>) 5.164</u>                |                                    | <u>(1,2,3,4)<sup>-</sup> 5.10</u> | <u>3<sup>-</sup> 5.110</u>                      |
| <u>(7<sup>±</sup>, 8<sup>+</sup>) 5.060</u> | (2) <u>4.99</u>                    | <u>(7<sup>+</sup>) 5.05</u>       | <u>(1<sup>-</sup>) 5.068</u>                    |
|   |                                    | <u>(1,2,3,4)<sup>-</sup> 4.98</u> |   |
|   | <u>4.82</u>                        | <u>(1,2,3,4)<sup>-</sup> 4.81</u> | <u>3<sup>-</sup> 4.817</u>                      |
|   | (2) <u>4.68</u>                    | <u>4.65</u>                       | <u>2<sup>+</sup> 4.683</u>                      |
|   | <u>4.54</u>                        | <u>(3<sup>+</sup>) 4.58</u>       | <u>6<sup>+</sup> 4.543</u>                      |
| <u>(7<sup>±</sup>, 6<sup>±</sup>) 4.542</u> | <u>4.47</u>                        | <u>(6<sup>+</sup>) 4.53</u>       | <u>0<sup>+</sup> 4.427</u>                      |
|   | <u>4</u> <u>4.33</u>               | <u>(5<sup>+</sup>) 4.44</u>       | <u>4<sup>+</sup> 4.335</u>                      |
|   | (2,5) <u>4.23</u>                  | <u>(4<sup>+</sup>) 4.32</u>       | <u>2<sup>+</sup> 4.232</u>                      |
| <u>(6<sup>-</sup>) 4.232</u>                | <u>4.12</u>                        | <u>(2<sup>+</sup>) 4.22</u>       | <u>0<sup>+</sup> 4.125</u>                      |
|   | (3) <u>4.07</u>                    |                                   |   |
|   | <u>5</u> <u>3.97</u>               |                                   |   |
|   | <u>2</u> <u>3.85</u>               |                                   |   |
| <u>8<sup>+</sup> 3.589</u>                  | <u>6</u> <u>3.45</u>               |                                   |   |
| <u>6<sup>+</sup> 3.448</u>                  | <u>2</u> <u>3.31</u>               |                                   |   |
| <u>4<sup>+</sup> 3.077</u>                  | <u>4</u> <u>3.09</u>               |                                   |   |
|   | <u>3</u> <u>2.74</u>               |                                   | <u>3<sup>-</sup> 2.748</u>                      |
| <u>5<sup>-</sup> 2.319</u>                  | <u>5</u> <u>2.32</u>               |                                   | <u>5<sup>-</sup> 2.319</u>                      |
| <u>2<sup>+</sup> 2.186</u>                  | <u>2</u> <u>2.18</u>               | <u>(2<sup>+</sup>) 2.184</u>      | <u>2<sup>+</sup> 2.186</u>                      |
| <u>0<sup>+</sup> 1.761</u>                  | <u>0</u> <u>1.75</u>               |                                   | <u>0<sup>+</sup> 1.761</u>                      |
| <u>0<sup>+</sup></u>                        |                                    | <u>(0<sup>+</sup>)</u>            | <u>0<sup>+</sup></u>                            |
| <sup>90</sup> Nb DECAY                      | <sup>90</sup> Zr ( $\rho, \rho'$ ) | <sup>91</sup> Zr ( $\rho, d$ )    | <sup>92</sup> Zr ( $\rho, t$ ) <sup>90</sup> Zr |

FIG. 8. Comparison of energy levels observed in <sup>90</sup>Zr. The present results are at the far right. The decay data are taken from Refs. 31 and 32, the  $(p, p')$  data from Ref. 30, and the  $(p, d)$  data from Ref. 2.

Since excitation of non-normal-parity states is allowed for the two-step  $(p, t)$  reaction,<sup>35</sup> we conclude that the two-step process does not contribute significantly to the transitions observed in this work.

#### E. Levels in $^{92}\text{Zr}$

The low-lying levels observed in the  $^{94}\text{Zr}(p, t)$  reaction are compared in Fig. 9 with results of other experiments.<sup>36-38</sup> All of the levels extracted from the present study have been reported with the exception of a possible weak state at 2.386 MeV. This level was observed at only a few angles and no  $L$  assignment can be made.

The present data are consistent with, but are not unique enough to confirm, the previous  $3^-$  assignments to the 2.341-MeV level. The present data yield a tentative assignment of  $5^-$  to the level at 2.485 MeV.

No other strongly populated levels are observed below 3.5 MeV of excitation. The high level density observed for the higher excited states precludes any meaningful analysis with the present experimental resolution.

A surprising feature of this reaction is the lack of any strength to the  $2^+$  level at 2.07 MeV. This level is populated strongly in the  $^{90}\text{Zr}(t, p)$  reaction.<sup>21</sup> We see no evidence for this level. Such behavior suggests that this state may contain a major component of  $[(2d_{5/2})(3s_{1/2})]$  structure that will not be populated strongly in the pickup reaction from  $^{94}\text{Zr}$ . The lack of any observable strength also suggests an accidental cancellation of terms contributing to this transition.

#### F. Levels in $^{94}\text{Zr}$

As in the preceding case, because of high level densities and the additional complication of large

| $J^\pi$                           | $\Delta L$                                      | $l_n$                                       | $J^\pi$                                     | $J^\pi$  |
|-----------------------------------|---|---|---|--|
| <u><math>(1,2)^+</math> 2.473</u> | <u>(5) 2.49</u>                                 |   | <u>2.491</u>                                | <u><math>(5^-)</math> 2.485</u>                        |
| <u><math>3^-</math> 2.340</u>     | <u>2.34</u>                                     | <u>2</u>                                    | <u><math>3^-</math> 2.346</u>               | <u>2.386</u>   |
|                                   |   | <u>2.390</u>                                |   | <u>2.341</u>   |
|                                   |   | <u>2.330</u>                                |   |  |
|                                   | <u>2.18</u>                                     | <u>2.150</u>                                |   |  |
| <u><math>(2,3)^+</math> 2.067</u> | <u>(2,4) 2.07</u>                               | <u>0 2.070</u>                              | <u><math>2^+</math> 2.071</u>               |  |
| <u><math>2^+</math> 1.847</u>     | <u>2 1.85</u>                                   | <u>2 1.840</u>                              | <u><math>2^+</math> 1.842</u>               | <u><math>2^+</math> 1.850</u>                          |
| <u><math>4^+</math> 1.496</u>     | <u>4 1.50</u>                                   | <u>2 1.495</u>                              | <u><math>4^+</math> 1.497</u>               | <u><math>4^+</math> 1.497</u>                          |
| <u><math>0^+</math> 1.383</u>     | <u>0 1.37</u>                                   |   | <u><math>0^+</math> 1.390</u>               | <u><math>0^+</math> 1.389</u>                          |
| <u><math>2^+</math> 0.935</u>     | <u>2 0.93</u>                                   | <u>2 0.930</u>                              | <u><math>2^+</math> 0.935</u>               | <u><math>2^+</math> 0.935</u>                          |
| <u><math>0^+</math> 0</u>         | <u><math>^{92}\text{Zr}(\rho, \rho')</math></u> | <u><math>^{91}\text{Zr}(d, \rho)</math></u> | <u><math>^{90}\text{Zr}(t, \rho)</math></u> | <u><math>^{94}\text{Zr}(p, t)^{92}\text{Zr}</math></u> |

FIG. 9. Comparison of low-lying energy levels in  $^{92}\text{Zr}$ . The present results are at the far right. The decay data are taken from Refs. 37 and 38, the  $(p, p')$  data from Ref. 30, the  $(d, p)$  data from Ref. 36, and the  $(t, p)$  data from Ref. 21.



target impurities, we have analyzed only the low-lying levels observed in the  $^{96}\text{Zr}(p, t)$  reaction. These are compared with other data on  $^{94}\text{Zr}$  in Fig. 10.

All of the levels we observe have been reported previously except the state at 2.152 MeV which we assign  $2^+$ . This level is fairly strongly populated in the present work while the  $2^+$  level at 2.371 MeV is less than half as intense. This latter state is strongly excited in the  $^{92}\text{Zr}(t, p)$  reaction.<sup>21</sup> Although they do not report a level at 2.152 MeV, the proton spectrum shown for this reaction appears to indicate a very weak peak at this energy.

Apparently there is some feature of the wave functions that produces a  $2^+$  level in  $^{92}\text{Zr}$  that can be easily populated in the  $^{90}\text{Zr}(t, p)$  reaction but not by  $^{94}\text{Zr}(p, t)$  and another  $2^+$  in  $^{94}\text{Zr}$  that can be easily populated by the  $^{96}\text{Zr}(p, t)$  reaction but not by  $^{92}\text{Zr}(t, p)$ .

#### G. Comparison with Extended Shell-Model Calculations

In the previous section we have listed enhancement factors for many of the observed transitions based on the assumption that the neutrons beyond  $N = 50$  occupy only the  $2d_{5/2}$  orbital. This does not imply that we assume such a model to be an adequate description of the low-lying states of these nuclei, but was done because it provided a convenient means of displaying relative transition strengths.

While the single neutron transfer studies on these nuclei show a preference for the neutrons to occupy the  $2d_{5/2}$  orbital, they also indicate significant occupation of the other orbitals in the  $N = 50$  to  $N = 82$  shell. Wave functions have been calculated which include the effect of some of these higher orbitals.

The details of the shell-model calculations will be presented elsewhere. Briefly, the calculations are based on an inert  $^{88}\text{Sr}$  core with two protons distributed in the  $2p_{1/2}$  and  $1g_{9/2}$  orbitals. The neutrons in excess of 50 were allowed to distribute themselves over the complete space of the  $2d_{5/2}$ ,  $2d_{3/2}$ , and  $3s_{1/2}$  orbitals. Single-particle energies were taken from experimental data and a phenomenological two-body interaction was employed to construct the energy matrices. The Oak Ridge-Rochester shell-model program<sup>39</sup> was used to calculate the wave functions and the nuclear overlap factors  $B(j_1 j_2 J)$ . These wave functions have been shown previously<sup>15</sup> to give a good description of the  $\text{Zr}(t, p)$  results, both for the relative ground-state-to-ground-state transitions and for the low-lying levels in each isotope.

The results for the present  $(p, t)$  work are

shown in Table IX. The enhancement factors obtained for the extended wave functions are calculated by inserting the  $B(j_1 j_2 J)$  values for the various components into the code JULIE and performing the multiple-configuration calculation as indicated in Eq. (1). The most striking feature of the enhancements calculated from the extended model is the good agreement for the ground-state transitions. The value of  $D_0^2 = 22$  that we have used throughout this paper was selected to make the  $^{94}\text{Zr}(p, t)$  enhancement factor unity. Thus, the relative enhancement factors have more significance than the absolute values. This value of  $D_0^2$ , however, falls within the limits established from previous studies. Within the accuracy of fitting the experimental angular distribution to the DWBA predictions, the ground-state-to-ground-state

|                         |                        |                                      |
|-------------------------|------------------------|--------------------------------------|
| $\Delta L$              | $J^\pi$                | $J^\pi$                              |
| (5) <u>2.61</u>         | <u>2.611</u>           | <u>5^- 2.603</u>                     |
| (2,4) <u>2.36</u>       | <u>2^+ 2.374</u>       | <u>2^+ 2.371</u>                     |
| (2) <u>2.32</u>         |                        |                                      |
| <u>2.16</u>             |                        | <u>2^+ 2.152</u>                     |
| 3 <u>2.06</u>           | <u>3^- 2.064</u>       | <u>3^- 2.060</u>                     |
| 2 <u>1.66</u>           | <u>2^+ 1.675</u>       | <u>2^+ 1.671</u>                     |
| 4 <u>1.47</u>           | <u>4^+ 1.471</u>       | <u>4^+ 1.469</u>                     |
| 0 <u>1.30</u>           | <u>0^+ 1.304</u>       | <u>0^+ 1.295</u>                     |
| 2 <u>0.92</u>           | <u>2^+ 0.920</u>       | <u>2^+ 0.920</u>                     |
| <u>0</u>                | <u>0^+ 0</u>           | <u>0^+ 0</u>                         |
| $^{94}\text{Zr}(p, p')$ | $^{92}\text{Zr}(t, p)$ | $^{96}\text{Zr}(p, t)^{94}\text{Zr}$ |

FIG. 10. Comparison of low-lying energy levels observed in  $^{94}\text{Zr}$ . The present results are at the far right. The  $(p, p')$  data are taken from Ref. 30 and the  $(t, p)$  data from Ref. 21.

TABLE IX. Comparison of  $(p, t)$  transition enhancements derived assuming a simple  $(d_{5/2})^n$  model with enhancements obtained from more complete shell-model wave functions. All enhancements are extracted for a value of  $D_0^2 = 22$ . The extent of disagreement with the model predictions can be judged by noting deviations of the enhancement factors from unity.

| Reaction                                    | $E(\text{MeV})$ | $J^\pi$ | $\mathcal{E}(d_{5/2})^n$ | $\mathcal{E}(\text{S.M.})$ |
|---|-----------------|---------|--------------------------|----------------------------|
| $^{92}\text{Zr} \rightarrow ^{90}\text{Zr}$ | 0.000           | $0^+$   | 1.6                      | 1.06                       |
| $^{94}\text{Zr} \rightarrow ^{92}\text{Zr}$ | 0.000           | $0^+$   | 1.7                      | 1.00                       |
|   | 0.935           | $2^+$   | 0.7                      | 0.6                        |
|   | 1.497           | $4^+$   | 0.7                      | 0.8                        |
|   | 1.850           | $2^+$   | 0.3                      | 2.2                        |
| $^{96}\text{Zr} \rightarrow ^{94}\text{Zr}$ | 0.000           | $0^+$   | 2.0                      | 1.01                       |
|   | 0.920           | $2^+$   | 0.9                      | 0.8                        |
|   | 1.469           | $4^+$   | 0.8                      | 1.0                        |
|   | 1.671           | $2^+$   | 0.08                     | 1.6                        |

transitions are very well accounted for by the extended model. This should not be too surprising, since the  $(p, t)$  intensities are mostly sensitive to the details of the neutron structure and should not be very dependent on the limited number of proton configurations used (two orbitals). The most obvious omission from the active neutron orbitals is the  $1g_{7/2}$ . This was omitted to reduce the size of the energy matrices and was justified by noting that the two-neutron pickup from this orbital will not contribute much intensity to the  $L=0$  transfers due to the details of the reaction mechanism. The omission of this orbital may be more serious for the other  $L$  transfers.

The low-lying weakly excited  $0^+$  levels are not shown in Table IX. These have been discussed previously as arising primarily from recoupling

of the proton configurations.<sup>23</sup> Such an interpretation seems consistent with the calculations within errors associated with predicting weak transitions. Experimentally these levels are down about 2 orders of magnitude from the ground-state intensity while the calculation predicts a 2 to 3 order-of-magnitude decrease for these transitions.

The model calculations do not seem to improve the agreement for the  $2^+$  levels. The tendency seems to be that more  $L=2$  strength is observed in higher excited levels than predicted. Thus, enhancements are less than unity for the first  $2^+$  and more than unity for the second  $2^+$  levels. The calculations produce improved agreement for the lowest  $4^+$  levels.

It seems obvious that rather complete wave functions will be required to obtain good agreement with the data. Although the results of the present calculation are encouraging, it seems necessary to include at least the  $1g_{7/2}$  orbital and some study needs to be made of the importance of "core-pickup" contributions to these low-lying states.

#### ACKNOWLEDGMENTS

The authors are indebted to R. M. Drisko for many helpful discussions throughout the course of this work. The careful plate scanning of V. Jones, R. Shelton, and M. P. Haydon is gratefully acknowledged. We would also like to acknowledge A. Pugh for his assistance in the data accumulation and the target fabrication group of the Oak Ridge National Laboratory isotopes division for their help in fabricating the thin targets.

\*Research sponsored by the U. S. Atomic Energy Commission under contract with the Union Carbide Corporation.

<sup>1</sup>B. L. Cohen and O. V. Chubinsky, Phys. Rev. **131**, 2184 (1963).

<sup>2</sup>J. B. Ball and C. B. Fulmer, Phys. Rev. **172**, 1199 (1968).

<sup>3</sup>J. B. Ball, R. L. Auble, R. M. Drisko, and P. G. Roos, Phys. Rev. **177**, 1699 (1969).

<sup>4</sup>A. Bohr, in *Proceedings of the International Conference on Nuclear Physics, Paris, 1964*, edited by P. Gutenberger (Centre National de la Recherche Scientifique, Paris, France, 1964), Vol. 1.

<sup>5</sup>D. R. Bes and R. A. Broglia, Nucl. Phys. **80**, 289 (1966).

<sup>6</sup>A. Bohr, in *Proceedings of the International Symposium on Nuclear Structure, Dubna, 1968* (International Atomic Energy Agency, Vienna, Austria, 1969); O. Nathan, *ibid.*

<sup>7</sup>R. R. Ries, R. A. Damerow, and W. H. Johnson, Jr.,

Phys. Rev. **132**, 1662 (1963).

<sup>8</sup>J. H. E. Mattauch, W. Thiele, and A. H. Wapstra, Nucl. Phys. **67**, 1 (1965).

<sup>9</sup>A. H. Wapstra and N. B. Gove, to be published.

<sup>10</sup>N. K. Glendenning, Phys. Rev. **137**, B102 (1965); B. F. Bayman, Argonne National Laboratory Report No. ANL-6878, 1964 (unpublished).

<sup>11</sup>R. M. Drisko, unpublished.

<sup>12</sup>S. Yoshida, Nucl. Phys. **33**, 685 (1962).

<sup>13</sup>A. de-Shalit and I. Talmi, *Nuclear Shell Theory* (Academic Press Inc., New York, 1963), p. 281.

<sup>14</sup>R. M. Drisko and F. Rybicki, Phys. Rev. Letters **16**, 275 (1966).

<sup>15</sup>E. R. Flynn, Bull. Am. Phys. Soc. **14**, 1197 (1969); and Los Alamos Scientific Laboratory Report No. LA-DC-10244 (unpublished).

<sup>16</sup>L. N. Blumberg, E. E. Gross, A. van der Woude, A. Zucker, and R. H. Bassel, Phys. Rev. **147**, 812 (1966).

<sup>17</sup>M. P. Fricke, E. E. Gross, B. J. Morton, and A. Zucker, Phys. Rev. **156**, 1207 (1967).

- <sup>18</sup>F. D. Becchetti and G. W. Greenlees, *Phys. Rev.* **182**, 1190 (1969).
- <sup>19</sup>R. M. Drisko, P. G. Roos, and R. H. Bassel, *J. Phys. Soc. Japan Suppl.* **24**, 347 (1968).
- <sup>20</sup>E. F. Gibson, B. W. Ridley, J. J. Kraushaar, M. E. Rickey, and R. H. Bassel, *Phys. Rev.* **155**, 1194 (1967).
- <sup>21</sup>J. G. Beery, Los Alamos Scientific Laboratory Report No. LA-3958, 1968 (unpublished).
- <sup>22</sup>F. G. Perey and A. M. Saruis, *Nucl. Phys.* **70**, 225 (1965).
- <sup>23</sup>J. B. Ball, R. L. Auble, and P. G. Roos, *Phys. Letters* **29B**, 172 (1969).
- <sup>24</sup>B. Sørensen, *Nucl. Phys.* **A134**, 1 (1969).
- <sup>25</sup>J. B. Ball, R. L. Auble, J. Rapaport, and C. B. Fulmer, *Phys. Letters* **30B**, 533 (1969).
- <sup>26</sup>J. Flegenheimer, *Radiochim. Acta* **6**, 21 (1966).
- <sup>27</sup>J. M. Jaklevic, C. M. Lederer, and J. M. Hollander, to be published.
- <sup>28</sup>R. C. Hagenauer, Ph.D. thesis, University of Tennessee, 1969 (unpublished); R. C. Hagenauer, E. Eichler, and G. D. O'Kelley, to be published.
- <sup>29</sup>K. P. Lieb and T. Hausmann, *Phys. Rev.* **186**, 1229 (1969).
- <sup>30</sup>J. K. Dickens, E. Eichler, and G. R. Satchler, *Phys. Rev.* **168**, 1355 (1968).
- <sup>31</sup>H. Pettersson, S. Antman, and Y. Grunditz, *Nucl. Phys.* **A117**, 241 (1968).
- <sup>32</sup>S. O. Simmons, Ph.D. thesis, Iowa State University, 1970 (unpublished); A. B. Tucker and S. O. Simmons, *Nucl. Phys.* **A156**, 83 (1970).
- <sup>33</sup>J. B. Ball, M. W. Johns, and K. Way, *Nucl. Data* **A8**, 407 (1970).
- <sup>34</sup>N. Freed and W. Rhodes, *Phys. Letters* **31B**, 45 (1970).
- <sup>35</sup>R. J. Ascuitto and N. K. Glendenning, *Phys. Rev. C* **2**, 1260 (1970).
- <sup>36</sup>J. K. Dickens and E. Eichler, *Nucl. Phys.* **A101**, 408 (1967).
- <sup>37</sup>M. E. Bunker, B. J. Dropesky, J. D. Knight, and J. W. Starner, *Phys. Rev.* **127**, 844 (1962).
- <sup>38</sup>W. L. Talbert, F. K. Wahn, H. H. Hsu, and S. T. Hsue, *Nucl. Phys.* **A146**, 149 (1970).
- <sup>39</sup>J. B. French, E. C. Halbert, J. B. McGrory, and S. S. M. Wong, in *Advances in Nuclear Physics*, edited by M. Baranger and E. Vogt (Plenum Press, Inc., New York, 1969), Vol. 3, pp. 193-257.

PHYSICAL REVIEW C

VOLUME 4, NUMBER 1

JULY 1971

## Radioactive Decay of 23-min <sup>131</sup>Sb to Levels of <sup>131</sup>Te

J. Blachot,\* H. N. Erten,† and C. D. Coryell

*A. A. Noyes Nuclear Chemistry Center, Massachusetts Institute of Technology, Cambridge, Massachusetts 02139†*

and

E. S. Macias

*Department of Chemistry, Washington University, St. Louis, Missouri 63130*

and

W. B. Walters

*Department of Chemistry, University of Maryland, College Park, Maryland 20742*

(Received 1 March 1971)

The levels of <sup>131</sup>Te have been investigated by studying the  $\gamma$  rays following the  $\beta$  decay of 23-min <sup>131</sup>Sb using Ge(Li) detectors. The <sup>131</sup>Sb sources were produced by rapid separation of Sb from <sup>235</sup>U thermal-neutron-fission products. 60  $\gamma$  rays attributed to <sup>131</sup>Sb decay have been observed and  $\gamma$ - $\gamma$  coincidence relationships have been obtained for the prominent lines. A level scheme has been constructed which incorporates 40 of these  $\gamma$  transitions between 23 levels in <sup>131</sup>Te. This level scheme is compared with the level structure of other odd-A Te isotopes and is discussed within the framework of the pairing-plus-quadrupole model.

### I. INTRODUCTION

The radioactive decay of fission-product <sup>131</sup>Sb has been difficult to characterize, as <sup>131</sup>Sb is usually isolated along with other Sb activities with similar half-lives.<sup>1</sup> Early studies indicated half-lives of 23 and 26 min.<sup>2,3</sup> Studies indicated half-spectra using NaI(Tl)<sup>4</sup> and Ge(Li)<sup>5</sup> detectors have revealed the presence of a number of  $\gamma$  rays. Be-

cause of the close half-life values of 40 and 5.7 min for <sup>130</sup>Sb isomers<sup>6</sup> and the growth of daughter<sup>7</sup> 25-min <sup>131</sup>Te, complex  $\gamma$ -ray spectra are observed and assignment of the weaker  $\gamma$  rays is difficult. We have used a high-resolution Ge(Li) detector, a buffer-memory coincidence system, and a fast magnetic-tape readout system<sup>7</sup> to identify many of  $\gamma$  rays and  $\gamma$ - $\gamma$  coincidence relationships present in the decay of <sup>131</sup>Sb. These data were used in con-